IMPACT DAMAGE ON SHIELDED GAS-FILLED VESSELS

F. Schäfer[(1)], E. Schneider[(1)], M. Lambert[(2)]

[(1)]Ernst-Mach-Institut – Fraunhofer Institut für Kurzzeitdynamik, Eckerstr. 4, D-79104, Freiburg, Germany, Email: schaefer@emi.fhg.de, schneider@emi.fhg.de

[(2)]ESA-ESTEC, Postbus 299, NL-2200 AG Noordwijk, The Netherlands, E-mail: michel.lambert@esa.int

ABSTRACT

This paper gives a summary of the findings from impacts on shielded gas-filled cylindrical aluminium alloy (Al2219 T851) and titanium alloy (Ti6Al4V) pressure vessels that were performed at the Ernst-Mach-Institute in the frame of an ESA contract [1]. The effect of impacts on shielded vessels with projectiles that have a kinetic energy close to the ballistic limit of the combined system of shield and vessel's front wall was investigated. The shields were single Al-bumper plates, unreinforced MLI and MLI reinforced with 2 layers of Betacloth. The threshold diameters that cause leakage from the vessel's front wall were determined experimentally as a function of shield material and shield spacing. For Al-shielded Al- and Ti-vessels, a safety design factor to avoid leakage is presented based on existing Whipple shield equations.

1. INTRODUCTION

Particle impacts on unshielded gas-filled pressure vessels can lead to gas leakage and catastrophic failure, if pressure and impactor energy exceed certain limit values [2] - [5]. Shielding of the vessels reduces the potential damage of catastrophic rupturing due to energy dissipation and fragmentation of the projectile upon impact on the bumper [1]. However, the overall risk for catastrophic rupturing of shielded or unshielded vessels placed aboard spacecraft in LEO upon impact is still low due to the low probability of occurrence of large debris particles. In contrast, the number of sub-millimeter and millimeter-sized space debris particles in LEO is enormously large, posing a threat to pressure containers stored aboard spacecraft. As in most cases the pressure containers are shielded, be it by MLI placed on top of the vessels or by Al-bumper shields, usually the maximum damage to be expected from impacts of millimeter and sub-millimeter sized projectiles on shielded gas-filled vessels is non-catastrophic, ranging typically from cratering without any further structural effects to leakage of gas from the vessels front wall. Impact of such projectiles is analyzed in this paper (Fig. 1).

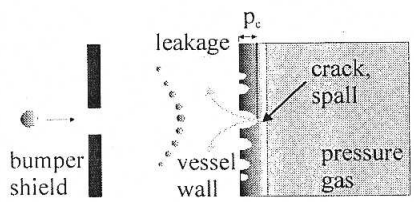

Fig. 1 Schematic: impact on shielded gas-filled pressure vessel at marginal perforation condition

2. TEST ARTICLES

2.1 Vessels

The pressure vessels were made from Al 2219 T851 and Ti6Al4V. The vessels were cylindrical with a L/D-ratio of 2.3. The thickness of the vessel walls was 1 mm, the inner diameter was 150 mm, and the length of the vessels was 350 mm (standard vessels). A few downscaled vessels were made from Al 2219. The scaling factor was 1:0.5 in length and diameter; the wall thickness remained 1 mm. The Al 2219 T851 vessels were manufactured from 18 mm thick plates of Al 2219 T351. The plates were machined down to the final tube wall thickness of 1.0 mm. Along two opposite edges, which were foreseen for the axial weld, a smooth transition to a narrow strip of twice the wall thickness was made to achieve reduced stresses along the axial welding joint. The plates were then bent to the desired vessel radius of 75 mm (resp. 37.5 mm for the downscaled vessels) and TIG welded along the axis. The vessels were finished by welding of the thick top cover ring plate and the bottom plate to the tube. Finally, the vessels were heat treated to yield the 851 temper. Resulting from the manufacturing process, deviations from the nominal wall thickness about ± 5% had to be accepted. The Ti6Al4V vessels were manufactured from nominally 1 mm thick rolled sheet material of annealed Ti6Al4V. They were bent to yield the desired radius and subsequently TIG welded along the axial ends. Finally the end plates were welded to the tube body. There was no heat treatment after welding.

A reference pressure was defined to provide a method for comparison between pressure vessels of different design and materials. This reference pressure is based on the definition of 'proof pressure', which is used in

pressure vessel design industry. It is based on a German standard [6] for the design of thin-walled cylindrical and spherical pressure vessels, based on the stress at 0.2% strain $R_{p0.2}$, the welding factor f_W, the safety design factor f_S, and geometrical factors:

$$p_{ref}[bar] = R_{p0.2}[MPa] \times (f_W/f_S) \times (t/R) \times 10$$

p_{ref} differs from the meaning of a proof pressure in that the corresponding pressure vessel has not been proof tested before the impact-test. Rather, it is assumed that this reference pressure is the technically maximum inflation pressure before the pressure vessel starts to fail. The safety design factor for titanium pressure vessels was chosen f_S =1.1, which is in accordance with [6]. The welding factor was set to f_W = 0.85. For aluminium alloy Al2219 pressure vessels, these factors amount to f_S =1.1 and f_W =0.55, respectively. The reference pressure for vessels from 1 mm thick annealed Ti6Al4V is p_{ref}=106.0 bar. As a result of the manufacturing process, the wall thickness of Al 2219 vessels showed slight variations. Thus the reference pressures for standard vessels from Al 2219 are in the range of p_{ref}=(38.3 ± 1.1) bar.

2.2 Shields

The shield materials were 1.0 mm thick plates of Al 5754, unreinforced Multi-Layer-Insulation blanket (MLI) and reinforced Multi-Layer-Insulation blanket (R-MLI). The unreinforced MLI blanket is shown in Fig. 2. The measured areal density was 0.056 g/cm^2. Reinforcement of the MLI was accomplished by placing two layers of Betacloth between the last Dacron layer and the rear cover layer (Nomex 487) of the MLI, as shown in Fig. 2 (areal density 0.111 g/cm^2).

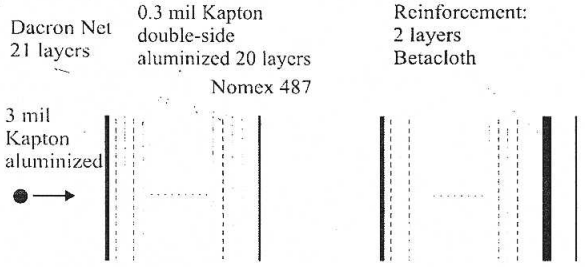

Fig. 2 Unreinforced MLI (left) and reinforced MLI

3. IMPACTS ON GAS-FILLED VESSELS

3.1 Shielded Al 2219 vessels

Four tests were performed on Al 2219 vessels that were shielded with 1 mm thick Al-plates (Table 1). The shield stand-off was 10 mm, 25 mm and 75 mm (Fig. 3). The impact velocities of all tests were around 7 km/s. The vessels were inflated with gaseous nitrogen. The wall stresses were between 165 and 219 MPa. The projectiles used were Al-spheres with a diameter of between 1.01 mm (10 mm spacing) and 2.5 mm (75 mm spacing). The maximum penetration depths in the vessel's front wall was 0.6 mm for the case of 75 mm spacing. No leakage of gas was recorded in the test samples.

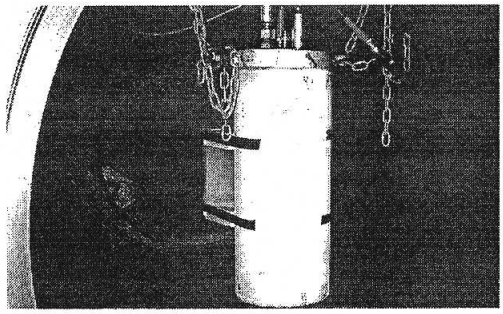

Fig. 3 Fully instrumented target setup; Al-shielded standard vessel at the EMI medium light gas gun. Perspective: look at the rear side of the vessel

Three impact tests were performed on MLI shielded vessels (Table 1). The shield had a stand-off of 10 mm and 25 mm. The wall stresses were between 165 and 213 MPa. For the lower shield spacing, impact of a projectile with a diameter of 1.01 mm did not lead to gas leakage, despite a maximum crater depth of 0.89 mm in the vessel's front wall. A slightly increased projectile diameter (1.10 mm) lead to gas leakage. At 25 mm stand-off, no leakage occurred from the surface of the vessel after impact of the 1.09 mm projectile.

shield t/S	EMI No.	d	v	$\alpha^{\S}$	p	σ_H	Damage #	p_c
[mm]		[mm]	[km/s]	[°]	[bar]	[MPa]		[mm]
Al 5754: 1/10	3573*	1.01	7.0	5	44.3	165	NL	0.40
Al 5754: 1/25	3503	1.4	6.9	12	30.5	205	NL	0.50
Al 5754: 1/25	3559*	1.41	6.9	40	55.4	207	NL	0.38
Al 5754: 1/75	3463	2.5	6.7	4	30.6	219	NL	0.60
MLI: 5/10	3844	1.01	7.1	8	29.9	210	NL	0.89
MLI: 5/10	3571*	1.10	7.1	2	43.6	165	L	-
MLI: 5/25	3555	1.09	7.2	3	29.6	213	NL	0.37
R-MLI: 5.3/10	3845	1.13	6.7	0	29.9	212	NL	0.26
R-MLI: 5.3/10	3843	1.25	6.6	5	30.6	225	L	-

§ impact angle on the surface of the vessel wall
* scale factor: 1:0.5 in L and D, 1:1 in t
# L=Leak detected; NL: no leak detected

Table 1 Results of all impact tests on shielded standard gas-filled Al 2219 vessels at around 7 km/s

The number of impact tests on reinforced MLI (R-MLI) shielded standard vessels was two (Table 1). Shield stand-off was 10 mm. The hoop stress in the

walls was 212 and 225 MPa. The first impact test was with a 1.13 mm Al-sphere, leading to a crater depth of 0.26 mm in the vessel's front wall (no leakage, Fig. 4). The second test was performed with a 1.25 mm Al-projectile. Perforation of the front wall of the vessel occurred, leading to gas leakage (Fig. 5). No cracks were formed in the rim of the impact hole.

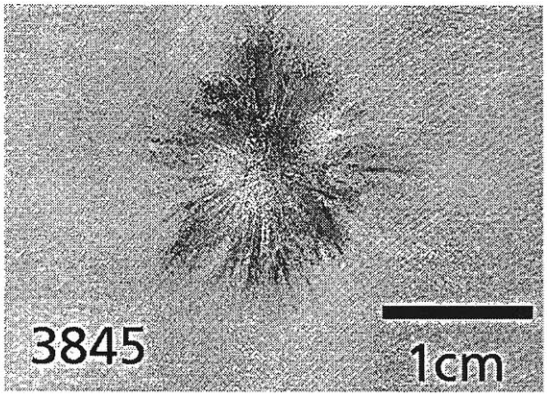

Fig. 4 Cratered front side of MLI shielded vessel in test 3845, no perforation, no leakage (Table 1)

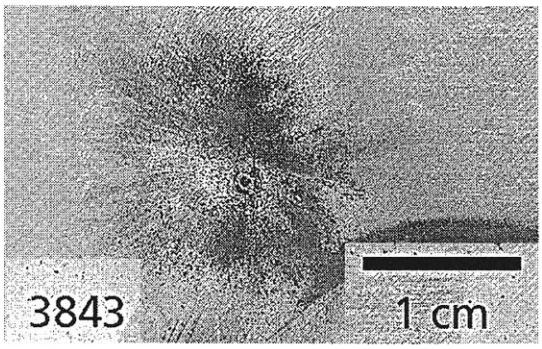

Fig. 5 Perforation hole in front side of MLI shielded vessel in test 3843 (Table 1)

3.2 Shielded Ti6Al4V vessels

A total of 5 shots were performed on nitrogen gas-filled Ti6Al4V vessels, which were shielded with a 1 mm thick Al bumper at a stand-off of 10 mm, 25 mm, and 75 mm (Table 2). Two of the vessels were inflated to 90 bar, which is about 85 % of the reference pressure. Three vessels were inflated to between 64.0 and 90.4 bar, corresponding to hoop stresses between 467 and 646 MPa. At 10 mm shield spacing, a maximum penetration depth of 0.31 mm was caused by a 1.58 mm diameter Al-projectile. The damage did not lead to leakage of gas from the vessel's surface. At 25 mm shield stand-off, the maximum penetration depth was 0.40 mm, leading to no leakage. At 75 mm shield stand-off, no leakage occurred after impact of the 3.5 mm Al-sphere, while the 3.94 mm Al-sphere caused a tiny leak that was only detected with the He-leak tester.

9 shots were performed on MLI shielded vessels, among them three shots at oblique impact (Table 2). The shield spacing was 0 mm, 10 mm, and 25 mm. The vessels were inflated to between 64.3 and 70.8 bar, corresponding to hoop stresses between 463 and 511 MPa. When the shield was placed directly on top of the vessel surface (spacing = 0 mm), even the smallest Al-projectile with a diameter of 0.9 mm perforated the vessel's front wall. At a moderate shield spacing of 10 mm, impact of a 1.32 mm diameter Al-sphere produced a small leak which was detected only by He- leakage testing, whereas the impact of a 1.1 mm diameter Al-sphere just produced a crater with a depth of 0.32 mm. At 25 mm shield spacing, no leakage occurred from the impact of a 1.20 mm projectile.

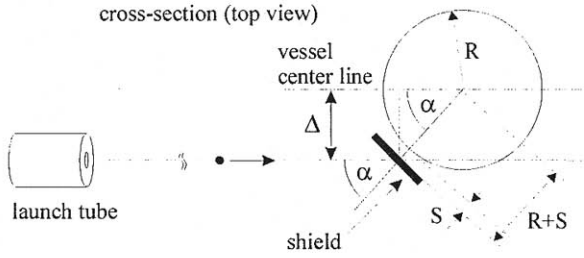

Fig. 6 Target set-up in oblique impact tests on shielded vessels from Ti6Al4V

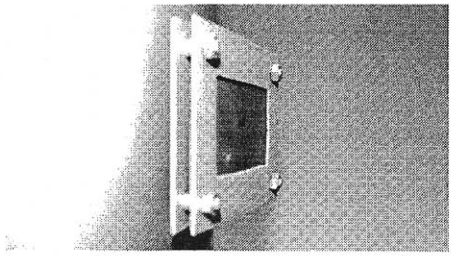

Fig. 7 Frame holder for the MLI fixed to the vessel (oblique impacts, side view)

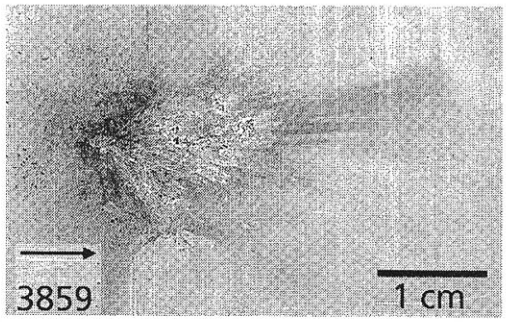

Fig. 8 Impact damage in vessel wall (oblique impact, MLI shield)

In the three oblique impact tests on MLI shielded vessel, the projectile impacted on the shield with an angle of obliquity of 45°. In order to achieve the oblique impact angle, the vessel was shifted laterally a distance Δ with respect to the shot axis (Fig. 6). Fig. 7

shows the vessel with the frame holder for the MLI. In subsequent impact tests the projectile diameter was increased from 1.25 mm to 1.54 mm. In none of the test, a leak was detected. The maximum penetration depth achieved was 0.49 mm (Fig. 8).

shield t/S	EMI No.	d	v	$\alpha^{\S}$	p	σ_H	Damage #	p_c
[mm]		[mm]	[km/s]	[°]	[bar]	[MPa]		[mm]
Al5754:1/10	3569*	1.58	6.8	$5^{\S}$	65.4	467	NL	0.31
Al5754:1/10	3846	1.73	7.1	$0^{\S}$	67.3	505	NL	0.27
Al5754:1/25	3515*	2.0	7.0	$7^{\S}$	90.0	643	NL	0.40
Al5754:1/75	3514*	3.5	7.1	$0^{\S}$	90.4	646	NL	0.50
Al5754:1/75	3952	3.94	7.1	$10^{\S}$	64.0	480	$L^{\$}$	0.55
MLI:5/0	3904	0.90	6.8	$9^{\S}$	66.5	499	L	-
MLI:5/0	3567	1.10	6.5	$12^{\S}$	68.5	489	L	-
MLI:5/0	3848	1.10	7.1	$0^{\S}$	66.8	501	L	-
MLI:5/10	3565	1.10	6.9	$5^{\S}$	64.8	463	NL	0.32
MLI:5/10	3850	1.32	7.3	$3^{\S}$	64.3	482	$L^{\$}$	0.60
MLI:5/25	3548	1.20	7.0	$12^{\S}$	70.8	506	NL	0.32
MLI:5/10	3858	1.25	6.8	$45^{\%}$	63.8	479	NL	0.31
MLI:5/10	3859	1.41	7.2	$45^{\%}$	64.8	486	NL	0.49
MLI:5/10	3905	1.54	7.2	$45^{\%}$	68.2	511	NL	0.35

§ impact angle on the surface of the vessel wall
$^{\$}$ leak was detected by He-leakage test
$^{\%}$ impact angle on the shield
* wall thickness 1.05 mm; all other vessels: 1.00 mm
# L=Leakage detected; NL: no leakage detected

Table 2 Results of all impact tests on shielded gas-filled Ti6Al4V vessels at around 7 km/s

4. ANALYSIS

Prior to performing the analysis, a definition of the usage of important terms is needed:

"Minimum safe diameter": The "minimum safe diameter" refers to the largest projectile diameter that did not cause leakage from the vessel's front wall. It is called "minimum" diameter, because the maximum possible projectile diameter that does not cause leakage might be larger by an amount to be determined by systematic experimental investigations only.

Definition of "failure": For the analysis of shielded vessels and Whipple shields, failure is defined in the following way: A vessel has failed when a leak is detected by Helium leakage tests.

4.1 Impacts on shielded Al 2219 vessels

Al-shields

Four impact tests have been performed at 3 different shield stand-offs. None of the tests resulted in leakage. The experimental projectile diameters plotted versus the stand-off of the shield in Fig. 9. Based on the experimental test results, an interpolating line was drawn that gives the minimum safe projectile diameter as a function of shield stand-off at impact velocities around 7 km/s.

If the impact of the projectile on the shielded vessel did produce craters in the vessel's front wall but did not cause leakage of gas, a useful approach to judge the safety margin is to compare the experimental projectile diameter i.e., the minimum safe projectile diameter, to the ballistic limit diameter for a Whipple shield that consists of a planar 1 mm thick Al-bumper and a planar backwall of Al 2219 of the same thickness as the vessel wall. The ballistic limit diameter is the limit projectile size for a given Whipple shield, where perforation of the back-up wall of the Whipple shield just occurs: As such, it is also the threshold projectile diameter for a shielded vessel that will lead to leakage of gas from the vessel's front side. Thus, the ballistic limit diameter of the equivalent Whipple shield was calculated as a function of spacing for a normal impact velocity of 7 km/s according to [7] (ballistic limit diameter of all-aluminium Whipple shields for $v_n \geq 7$ km/s). The ballistic limit curve is drawn into Fig. 9. Comparing the calculated curve to the experimental safe diameters, it is obvious that for the case of 10 mm stand-off, there is a margin of about 30 % on the projectile diameter in order to reach the ballistic limit, which is about the same for the 25 mm stand-off. At 75 mm stand-off, the calculated ballistic limit diameter is 2.59 mm, thus just about 4 % larger than the experimentally determined safe projectile diameter of 2.5 mm. Assuming that the ballistic limit curve is valid for the configurations under investigation i. e., provides the actual ballistic limit diameters, it can be stated that the impacted projectile diameters thus were very close to the calculated ballistic limit diameters of the corresponding Whipple shields.

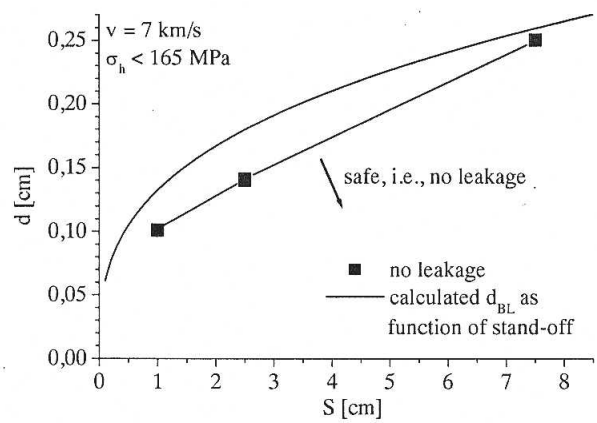

Fig. 9 Impacts on gas-filled Al-shielded Al-vessels; minimum limit diameter for safe operation regime as a function of shield-stand-off

MLI/R-MLI-shields

The projectile diameters are plotted in Fig. 10 versus the stand-off of the MLI/R-MLI shield. An interpolating line was drawn between the minimum safe projectile diameters for MLI shielding at 10 mm and 25 mm stand-off. The minimum safe diameter for MLI shields is 1.0 mm at 10 mm stand-off and 1.1 mm at 25 mm stand-off. For the MLI shielding, data exist from just one stand-off at 10 mm. The minimum safe diameter for this case is 1.13 mm; it is indicated in the diagram. In order to estimate how close the experimentally determined minimum safe diameters are to the actual projectile diameter that would cause leakage, the penetration depths of the deepest craters in the Al 2219 vessel wall were added to the data points. While the crater depth was fairly small for the test case involving the R-MLI shield at 10 mm stand-off (0.26 mm), the measured crater depth of 0.89 mm for the MLI shielded vessel at 10 mm stand-off indicates that failure would have occurred for a slightly larger projectile diameter.

Comparing the minimum safe projectile diameter for MLI and R-MLI shielding at 10 mm stand-off, a 13 % increase in diameter is achieved for the R-MLI shielding, which amounts to about an improvement of 40 % in terms of projectile mass.

It was attempted to calculate the ballistic limit diameter of the Whipple shield arrangement consisting of MLI or R-MLI bumper and Al 2219-backwall at various stand-offs according to [7] (ballistic limit diameter of all-aluminium Whipple shields for $v_n \geq 7$ km/s). The equations provided in [7] are - strictly speaking - only valid for Whipple shields consisting of Al-bumpers and Al-backwalls, taking into account some restrictions with respect to the S / d_p - and $(t_b * \rho_b) / (d_p * \rho_p)$ - ratios. However, the basic functional dependence of the various target and projectile parameters on the ballistic limit projectile diameter of a Whipple shield configuration has often been used in literature to estimate the ballistic limit diameters also for Whipple shields made from other materials. The same procedure is followed here.

To this purpose, the equivalent Al-bumper thickness was calculated from the areal density of the MLI. The equivalent Al-bumper thickness for the MLI is 0.207 mm, for the R-MLI it is 0.411 mm. The bumper density which is required by the ballistic limit equation in [7] was set equal to the density of Aluminium (i.e., 2.7 g/cm^3). For the backwall, the yield strength of Al 2219 was used. The calculated ballistic limit diameters of the MLI/Al2219- and R-MLI/Al 2219 Whipple shields are plotted into Fig. 10. Just one ballistic limit curve was drawn into the diagram, because the equation in [7] doesn't consider the bumper thickness for normal impact velocities above 7 km/s. Thus, the ballistic limit equation from [7] is of no use for the prediction of the ballistic limit diameters of Whipple shield arrangements consisting of MLI bumpers and Al-backwalls for the following reasons:

- the calculated ballistic limit diameters are at least 50% too large with respect to the experimental data at 10 mm stand-off; the predicted limit diameter of roughly 1.8 mm at 25 mm stand-off appears extremely overestimated considering the impact test results from the MLI bumper at 25 mm stand-off
- the equation doesn't consider the actual bumper thickness for normal impact velocities above 7 km/s, which is not in accordance with the test results for MLI and R-MLI shielding (this is true at least for a shield stand-off of 10 mm)

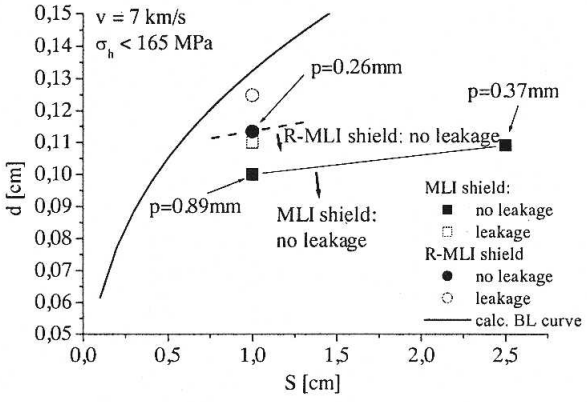

Fig. 10 Impacts on gas-filled MLI- and R-MLI shielded Al-vessels; minimum limit projectile diameter for no-leakage requirement as a function of shield stand-off

Safe operation regime for shielded Al 2219 vessels

The experimental finding that slightly impact-damaged Al 2219 vessels did not leak gas, even at high pressures and corresponding high wall stresses, is represented in Fig. 11. The maximum crater depth, normalized by the wall thickness, is plotted on the vertical axis. Pressure, normalized by the reference pressure, is plotted on the horizontal axis. In none of the corresponding experiments, leakage was recorded after the impact test or micro-cracks were identified. The maximum crater depth of roughly up to 60 % of the wall thickness at wall stresses up to 225 MPa, for which no leakage occurred, demonstrates the huge damage tolerance of the highly stressed vessel walls. Assuming that no leakage occurs from shallower craters or reduced hoop stresses, a safe operation regime can be identified. The limit lines of the experimentally characterized safe operation regime mark just the lower boundaries for both crater depth and pressure.

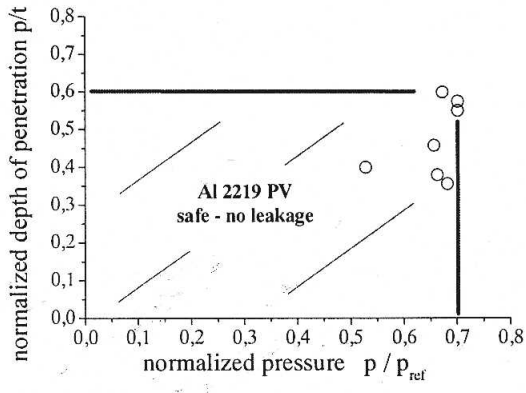

Fig. 11 "Safe operation regime" for shielded Al 2219 vessels

4.2 Impacts on shielded Ti6Al4V vessels

Five tests were performed on gas-filled Ti6Al4V vessels that were shielded with 1 mm thick Al-plates. In four out of the five tests no leakage occurred. The diameters of the projectiles that were used are plotted in Fig. 11 versus the shield stand-off. Based on the four experimental test results, in which the impacting projectile did not produce any leaks in the vessel wall at the various stand-offs, an interpolating line was drawn that gives the minimum safe projectile diameter as a function of shield stand-off at an impact velocity of 7 km/s. The largest possible safe projectile diameters might be slightly above the interpolated line. The margin between the experimentally determined safe projectile diameter and the maximum possible safe projectile diameter can be estimated, as was done with the Al-shielded Al 2219 vessels. In order to do so, the ballistic limit diameter for Whipple shields consisting of a planar Al-bumper shield and a planar backwall of Ti6Al4V of the same thickness as the vessel wall was calculated as a function of spacing for a normal impact velocity of 7 km/s according to [7] (ballistic limit diameter of all-aluminium Whipple shields for $v_n \geq 7$ km/s). The curve is drawn into Fig. 12. Any projectile diameter above the ballistic limit diameter perforates the backwall of the Whipple shield i.e. results in failure of the back-up wall. Considering this, the ballistic limit curve also represents an upper limit for the safe projectile diameter. Thus, for the case of 10 mm stand-off, there is a margin of about 3 % on the projectile diameter in order to reach the ballistic limit curve, while for the 25 mm stand-off, the margin on the safe projectile diameter is about 30 %. At 75 mm stand-off, the ballistic limit diameter was determined experimentally to between 3.5 mm and 3.94 mm, which is confirmed by the calculated ballistic limit curve. The calculated ballistic limit diameter is 3.67 mm, thus about 5 % larger than the experimentally determined safe projectile diameter of 3.5 mm.

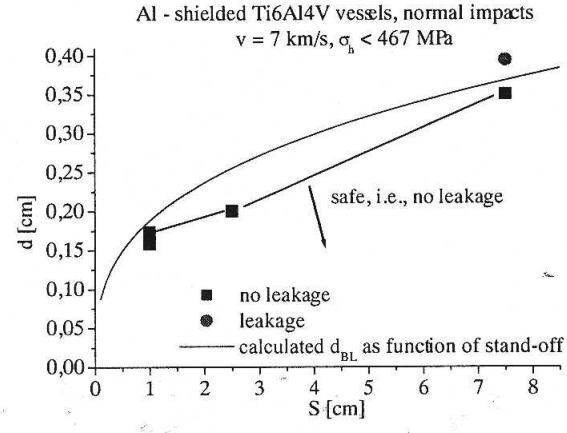

Fig. 12 Impacts on gas-filled Al-shielded Ti-vessels; minimum limit diameter for safe operation regime as a function of shield-stand-off

A total of 9 shots were performed on MLI-shielded gas-filled Ti-vessels, among them 3 at 45° incidence. The shield stand-off was varied between 0 mm and 25 mm. The projectile diameters are plotted in Fig. 13versus the shield stand-off. At 0 mm stand-off the minimum safe projectile diameter was not determined, because at the smallest projectile diameter of 0.9 mm leakage of gas occurred. At 10 mm and 25 mm, the minimum safe projectile diameters were determined. At 45°, even the largest projectile diameter didn't result in leakage. For the 0° shots, an interpolating line was drawn between the minimum safe projectile diameters at 10 mm and 25 mm stand-off. Below stand-offs of 10 mm, the "safe" operation domain was not be identified (it is indicated by a "?").

The results of the oblique impact tests are also added to the diagram. As can be seen, for 10 mm stand-off, the threshold projectile diameter that leads to leakage was not identified. Projectile diameters up to 1.54 mm at 7 km/s do not cause leakage of gas from the vessel wall when impacting at 45°.

Here also, it was attempted to calculate the ballistic limit diameter of the Whipple shield arrangement consisting of MLI bumper and Ti6Al4V-backwall at various stand-offs according to [7] (ballistic limit diameter of all-aluminium Whipple shields for $v_n \geq 7$ km/s). To this purpose, the equivalent Al-bumper thickness was calculated from the areal density of the MLI. It amounts to 0.207 mm. The bumper density needed in the equations was set equal to the density of Aluminium (i.e., 2.7 g/cm^3). For the backwall, the yield strength of the Ti-alloy was used. The calculated ballistic limit diameters of the MLI/Ti-Whipple shield are plotted into Fig. 13 for two impact angles of 0° and 45°. Comparing the calculated ballistic limit curves with the experimental results, it can immediately be stated that the equations from [7] cannot be applied to

the present case for the prediction of the ballistic limit diameters. It is also obvious that a single constant multiplication factor to the ballistic limit diameter equation will not be able to take into account the angular dependence of the ballistic limit diameter, because the 0° curve exceeds the 45° curve at 10 mm stand-off, whereas the situation is vice versa for stand-offs below approximately 6 mm.

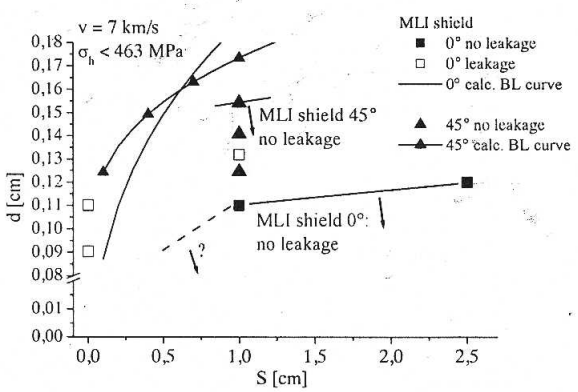

Fig. 13 Impacts on gas-filled MLI-shielded Ti-vessels; minimum limit projectile diameter for safe operation regime as a function of shield stand-off

In Fig. 14, the minimum safe projectile diameter for the case of an MLI shield at a stand-off of 10 mm was plotted versus impact angle. The safe diameter at 0° is 1.10 mm, at 45° it is 1.41 mm. An interpolating line was drawn to indicate the safe operation regime as a function of impact angle at 10 mm stand-off.

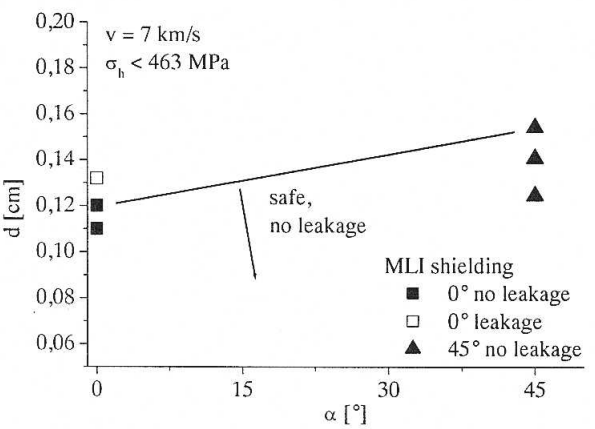

Fig. 14 Impacts on gas-filled MLI-shielded Ti-vessels; minimum limit projectile mass for safe operation regime as a function of impact angle (10 mm stand-off)

Safe operation regime for shielded Ti6Al4V vessels

Slightly impact-damaged Ti6Al4V vessels can be operated safely without leaking gas, even at high pressures. This finding is presented in Fig. 15, where the normalized maximum crater depth and normalized pressure are plotted on the vertical respectively the horizontal axis. In none of the added test data gas leakage occurred from the vessel's damaged front surface. A safe operation regime is plotted in the graph. The boundaries represent minimum safe crater depths and pressures, respectively.

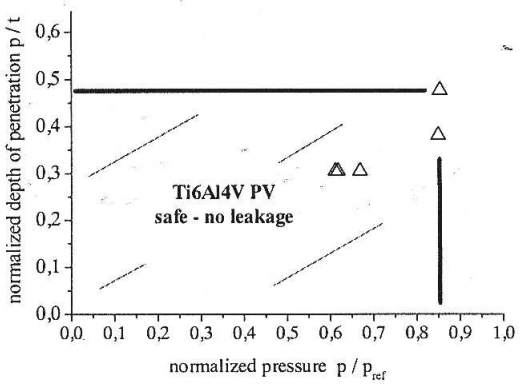

Fig. 15 "Safe operation regime" for Ti6Al4V vessels

5. CONCLUSIONS

For shielding with MLI, R-MLI and 1 mm thick Aluminium, the minimum safe diameter was determined for Al 2219 and Ti6Al4V vessels at various shield stand-offs at an impact velocity of 7 km/s. It was shown that the minimum safe diameter is almost a linear function of shield stand-off for stand-offs between 10 mm and 75 mm.

Small non-perforating impact damages in the front wall of the Al 2219 and Ti6Al4V pressure vessels under investigation do not lead to gas leakage, despite hoop stresses of up to 219 MPa and 646 MPa, respectively. This was confirmed experimentally for an impact velocity of around 7 km/s and a maximum penetration depth in the Al 2219/Ti6Al4V vessel wall of ca. 60 % resp. ca. 50 % of the vessel's wall thickness.

The shield effectiveness of the considered aluminium shields is a strong function of the stand-off, when placed in front of vessels made from Al 2219 and Ti6Al4V vessels. It was demonstrated that MLI, having just 20 % of the areal density of 1 mm thick aluminium, is an effective shielding material for both vessel materials.

If the front wall of the investigated Al 2219 and Ti6Al4V vessels are perforated and the hole diameter is just the size of a puncture, the vessel will not rupture catastrophically and no cracks will form in the rim of the perforation hole.

For Al-shielded Al 2219 and Ti6Al4V vessels, the experimentally determined minimum safe diameters

can be expressed as a fraction of the calculated ballistic limit diameters of the equivalent planar Whipple shield configurations from [7]. These fractions amounts to between 76% and 96% for Al 2219 vessels and between 76% and 97% for Ti6Al4V vessels.

The semi-analytical ballistic limit formulas for metal Whipple shield configurations presented in [7] are useful for an approximate determination of threshold impact parameters that do lead to leakage of gas, but do not predict the maximum penetration depths in the backwall plate required in this study nor do consider MLI or R-MLI as shield material. Thus impact tests are inevitable. Considering the importance of MLI as shielding material for spacecraft components and the various applications of MLI aboard spacecraft, an engineering equation that is capable to describe the ballistic limit of a Whipple shield consisting of a MLI bumper and an Al- or Ti-backwall is needed.

6. ACKNOWLEDGEMENT

This study was performed under ESA Contract 10556/93.

7. REFERENCES

1. Schäfer F., Hypervelocity Impact Testing, Impacts on Pressure Vessels, *Final Report to ESA Contract 10556/93*, EMI E 14/01, Ernst-Mach-Institut, Freiburg, Germany, February 2001.

2. Schäfer F., Schneider E., and Lambert M., Hypervelocity Impacts on Cylindrical Pressure Vessels - Experimental Results and Damage Classification, *Proc. 1997 ASME Pressure Vessels and Piping Conference*, Structures under Extreme Loading Conditions, July 27-31, 1997, Orlando, Florida, USA, PVP-Vol. 351, pp 235 - 244, The American Society of Mechanical Engineers 1997

3. Schäfer F., Schneider E., and Lambert M., An Experimental Study To Investigate Hypervelocity Impacts on Pressure Vessels, *Proc. Second European Conference on Space Debris*, 17-19 March 1997, ESOC, Darmstadt, Germany, ESA SP-393, pp 435 - 443, European Space Agency 1997

4. Whitney J. P., White P. D., Designing Hypervelocity Impact Testing for Thin-Walled Pressure Vessels, *43rd Meeting of the Aeroballistics Range Association*, Columbus, Ohio, Sep.1992.

5. Lambert M., Hypervelocity Impact on Pressure Vessels. An Overview, *European Space Agency*, Technical Note: YME/ML/1140, Oct.1991

6. German standard 'AD-Merkblätter' No's B0 and B1

7. Christiansen E. L., Design and Performance Equations for Advanced Meteoroid and Debris Shields, *Int. J. Impact Engng.* Vol.14, pp.145-156, 1993